Chinese Physics Letters **41**, 047103 (2024) **Express Letter**

Theory for Charge Density Wave and Orbital-Flux State in Antiferromagnetic Kagome Metal FeGe

Hai-Yang Ma(马海洋)[1,2,3], Jia-Xin Yin(殷嘉鑫)[4], M. Zahid Hasan[4,5,6], and Jianpeng Liu(刘健鹏)[1,2,7*]

[1]*School of Physical Science and Technology, ShanghaiTech University, Shanghai 201210, China*
[2]*ShanghaiTech Laboratory for Topological Physics, ShanghaiTech University, Shanghai 201210, China*
[3]*Quantum Science Center of Guangdong-HongKong-Macao Greater Bay Area, Shenzhen 518045, China*
[4]*Laboratory for Topological Quantum Matter and Advanced Spectroscopy (B7), Department of Physics, Princeton University, Princeton, New Jersey 08544, USA*
[5]*Princeton Institute for Science and Technology of Materials, Princeton University, Princeton, New Jersey 08544, USA*
[6]*Materials Sciences Division, Lawrence Berkeley National Laboratory, Berkeley, California 94720, USA*
[7]*Liaoning Academy of Materials, Shenyang 110167, China*

(Received 25 January 2024; accepted manuscript online 19 March 2024)

We theoretically study the charge order and orbital magnetic properties of a new type of antiferromagnetic kagome metal FeGe. Based on first-principles density functional theory calculations, we study the electronic structures, Fermi-surface quantum fluctuations, as well as phonon properties of the antiferromagnetic kagome metal FeGe. It is found that charge density wave emerges in such a system due to a subtle cooperation between electron–electron interactions and electron–phonon couplings, which gives rise to an unusual scenario of interaction-triggered phonon instabilities, and eventually yields a charge density wave (CDW) state. We further show that, in the CDW phase, the ground-state current density distribution exhibits an intriguing star-of-David pattern, leading to flux density modulation. The orbital fluxes (or current loops) in this system emerge as a result of the subtle interplay between magnetism, lattice geometries, charge order, and spin-orbit coupling (SOC), which can be described by a simple, yet universal, tight-binding theory including a Kane–Mele-type SOC term and a magnetic exchange interaction. We further study the origin of the peculiar step-edge states in FeGe, which sheds light on the topological properties and correlation effects in this new type of kagome antiferromagnetic material.

DOI: 10.1088/0256-307X/41/4/047103

The frustrated nature of a kagome lattice can give rise to intriguing electronic structures such as flat bands, Dirac cones, and van Hove singularities (VHS).[1–4] The flat bands may serve as a good platform for strongly correlated physics such as quantum magnetism and unconventional superconductivity.[5–12] The Dirac points can be gapped out by either spontaneous time-reversal symmetry breaking or spin-orbit coupling (SOC), which thus exhibits nontrivial topological properties.[8,9,13] When the Fermi level is tuned to the van Hove singularity of a kagome metal, various correlated states may emerge through the Fermi-surface nesting scenario as driven by electron–electron (e–e) Coulomb interactions.[14–28]

Recently, scanning tunneling microscopy and muon spin relaxation (μsR) measurements reveal time-reversal breaking charge orders in AV_3Sb_5 (A = K, Rb, Cs),[18,22,26,28] which emerge at temperatures near or below the 2×2 charge density wave (CDW) transitions for this class of materials. Interestingly, these time-reversal breaking CDW phases are proposed to exhibit spontaneous real-space current loops, and are associated with orbital flux patterns.[15,29–33] Moreover, recent experimental studies demonstrate that an antiferromagnetic metal FeGe with a kagome lattice structure also hosts a 2×2 charge order,[34,35] which is closely correlated with the antiferromagnetism.[36,37] Despite different theoretical proposals,[38–40] the origin of CDW state and how the charge order interplays with antiferromagnetism in FeGe are still open questions.

In this Letter we theoretically study the properties of charge density wave and the orbital-flux states in antiferromagnetic kagome metal FeGe. Based on first-principles density functional theory (DFT) calculations, we systematically investigate the electronic structures, Fermi-surface quantum fluctuations, and phonon properties of FeGe. Specifically, through generalized susceptibility calculations within random phase approximation (RPA), we find that e–e interactions alone cannot drive any CDW-type instability in FeGe. However, e–e interactions would renormalize the effective mass around the Fermi surface, which thus enhances the density of states contributed by Ge p orbitals. The latter is coupled with a branch of low-frequency optical phonon modes around M point, which consist of Ge atomic displacements. This branch of Ge phonon modes is getting softer with the increase of U as more and more Ge $4p$ orbitals contribute to the Fermi surface, and eventually becomes frozen with the onset of CDW. Therefore, we propose that the CDW state in FeGe is triggered by an interaction-assisted phonon instability.

We further show that, in the CDW phase, the inter-site

*Corresponding author. Email: liujp@shanghaitech.edu.cn
© 2024 Chinese Physical Society and IOP Publishing Ltd

currents in the ground state form a mutually intercalated star-of-David and double-triangular current pattern. Such orbital fluxes (or current loops) in this system emerges as a result of the subtle interplay between magnetism, lattice geometries, charge order, and SOC, which can be described by a simple, yet universal, tight-binding model including a Kane–Mele-type SOC term and a magnetic exchange interaction. Moreover, we have also studied FeGe in the monolayer form in the 2×2 CDW phase, which turns out to be a topological metal with both Weyl points and flat Chern band near the Fermi level, exhibiting multiple low-energy edge states. This naturally explains the origin of the recently observed spin polarized step-edge states in FeGe.

FeGe consists of an alternating stacking of the Fe_3Ge kagome layer and the Ge honeycomb layer as shown in Fig. 1(a). It has an A-type collinear antiferromagnetic order along the c axis which doubles the primitive cell with a Néel temperature $\sim 400\,\mathrm{K}$.[41] We perform DFT calculations with additional Hubbard-like on-site interactions applied to the Fe $3d$ orbitals, where the Hubbard U is treated as a parameter to be varied. With $U = 4.1\,\mathrm{eV}$ (determined through the linear-response method[42]) and Hund's coupling $J = U/5 = 0.82\,\mathrm{eV}$, the calculated local magnetic moment for each Fe atom is $2.61\,\mu_\mathrm{B}$. The band structures in the antiferromagnetic phase of the pristine structure are shown in Fig. 1(b), which involve multiple bands around the Fermi level. Moreover, these low-energy bands are topologically nontrivial, which host multiple Dirac nodal loops as marked by the green circles in Fig. S1 in the Supplementary Information (SI). The nodal loops are resided within the $k_z = \pi$ plane, which are protected by horizontal mirror symmetry. More details about the band topology are given in the SI.

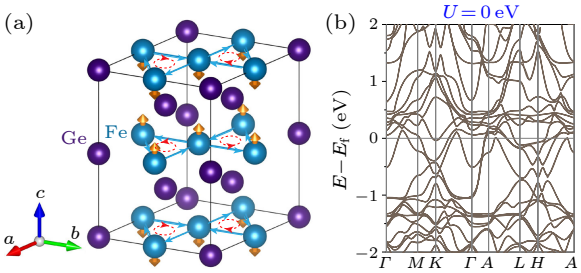

Fig. 1. Lattice structure, current patterns, and band structures of pristine FeGe. (a) Lattice structure and current patterns. The inter-site current flows are indicated by solid arrows, while the current loops among the Fe triangles are illustrated by the arrowed dash circles. (b) Band structures at $U = 0\,\mathrm{eV}$, with SOC included.

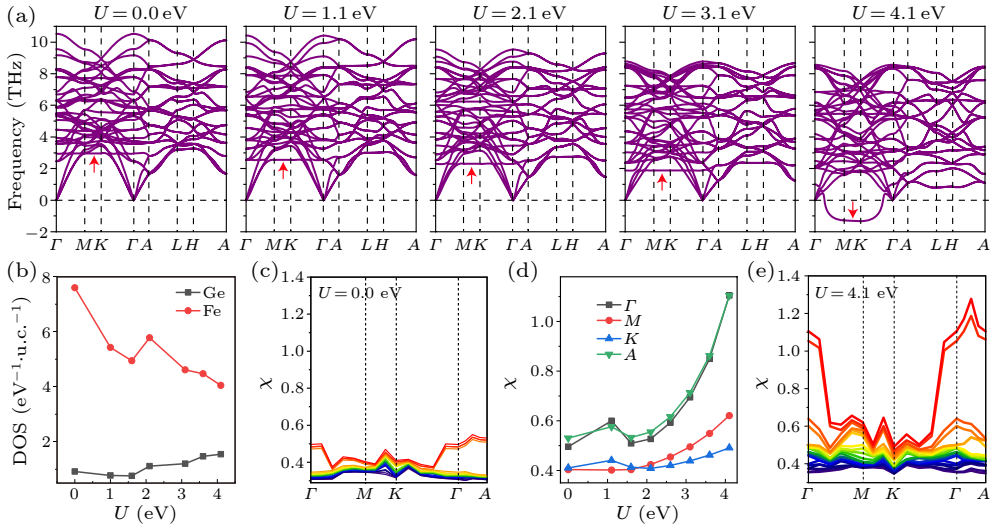

Fig. 2. (a) Phonon spectra at different on-site U. The flat bands which go down with increasing U are indicated by red arrows. (b) Dependence of the density of states (DOS) of Ge and Fe on U taken at the Fermi energy, in units of eV^{-1} per unit cell (u.c.). (c) Leading eigenvalues of the susceptibility tensors along a high-symmetry $\boldsymbol{q}$ path, taken at $U = 0.0\,\mathrm{eV}$. (c) Leading eigenvalues of the RPA susceptibility tensors of pristine FeGe at different Hubbard U values. (d) Dependence of the leading eigenvalues at the high-symmetry points on U. (e) The same as (c), but taken at $U = 4.1\,\mathrm{eV}$. Here $J = 0\,\mathrm{eV}$ for $U = 0\,\mathrm{eV}$ and $J = 0.82\,\mathrm{eV}$ otherwise.

We continue to discuss the origin of the CDW phase in FeGe. Recent experiments report an in-plane 2×2 charge order at temperatures below $\sim 100\,\mathrm{K}$ in FeGe, which seems to be intertwined with its antiferromagnetic order.[34] To shed light on the experiments, we first calculate the phonon spectra of pristine FeGe at different Hubbard U values, the results are shown in Fig. 2(a). As we can see, at small U, the phonon spectrum of the pristine structure is well behaved without any imaginary frequency, indicating that the pristine structure is stable. With the increasing U, a flat phonon band within the $k_z = 0$ plane, as marked by red arrow in Fig. 2(a), gradually moves downward in frequency and becomes imaginary when $U > 3.1\,\mathrm{eV}$, indicating that the pristine structure eventually gets unstable at larger U values, possibly with the onset of CDW. A closer inspection reveals that the soft branch of phonon modes is contributed by collective displacements of the Ge atoms. This unusual dependence of the phonon spectrum on the Hubbard U implies that the CDW transition in FeGe may be triggered by e–e interactions. It turns out

that with the increase of U, the flat bands contributed from the Fe 3d orbitals are gradually pushed away from the Fermi level (see Fig. S2 in the SI); meanwhile, contributions from the Ge 4p orbitals at the Fermi level become more and more significant [Fig. 2(b)] with the increase of U. As the soft phonon band [marked in Fig. 2(a)] is contributed by Ge displacements, it is coupled to the Ge 4p orbitals much more strongly than to the Fe 3d orbitals. Thus, an enhancement of the Ge 4p spectral weight at the Fermi surface would yield stronger electron–phonon coupling matrix elements for the soft phonon band with the Ge displacements. This would give rise to a strong renormalization effect to the phonon frequency,[43] and eventually makes the soft phonon band (from Ge displacements) unstable, driving the CDW transition. Such an argument is also consistent with the relaxed structure of the 2×2 CDW phase as shown in Fig. 3(a), in which only the Ge atoms show substantial distortions. We will discuss this in detail later.

We note that the Hubbard U value can be calculated self-consistently through the response process of local charge density to a perturbative potential,[42] which gives $U = 4.1\,\text{eV}$ for Fe 3d orbitals. This justifies the above argument that CDW of FeGe may be induced through an interaction-assisted phonon instability scenario. Certainly DFT+U is a mean-field approach which cannot fully capture the characteristics of single-particle excitation spectrum for such correlated metals. However, recently both angle resolved photoemission spectroscopy (ARPES) measurements[33] and DFT + dynamical mean field theory (DMFT) calculations[37] suggest an overall effective mass renormalization by a factor of ~ 1.6 compared to DFT band structures, with well defined quasi-particle features around Fermi level. As the Fermi surface has contributions from both Fe 3d and Ge 4p orbitals, both the overall density of states (DOS) and Ge 4p DOS around the Fermi level would be enhanced due to e–e interaction effects. This further confirms the above scenario that interaction-enhanced DOS would lead to stronger electron–phonon coupling effects thus induces phonon instability. We note that in Ref. [37], the CDW order is reported to be attributed to spin-phonon coupling mechanism, with significant phonon linewidth broadening observed between the magnetic and CDW transition temperature.

We also consider the possibility that the CDW state in antiferromagnetic FeGe may be driven by Fermi-surface instabilities due to strong e–e interaction effects. We calculate the general susceptibility tensor defined in the charge-sublattice-orbital-spin space[33] based on a realistic Wannier tight binding model including all the Fe 3d orbitals and Ge 4p orbitals generated from DFT calculations. The eigenmodes and eigenvalues of the static susceptibility tensor reflect the properties of the intrinsic quantum fluctuations at the Fermi surface. The e–e interaction renormalization effects on the generalized susceptibility tensor are treated by RPA. The leading eigenmodes of the RPA generalized susceptibility tensor indicate the possible spontaneous symmetry breaking states driven by Fermi surface quantum fluctuations and e–e interactions. The details are given in the SI. In Fig. 2(c), we show the eigenvalues of the bare susceptibility tensor calculated from the $U = 0$ Fermi surface in the antiferromagnetic ground state of FeGe with pristine lattice structure. We see that the eigenvalues of all the leading Fermi-surface fluctuation modes are small, with amplitudes $\lesssim 0.5$. Including e–e interactions in the RPA framework does not change the result qualitatively. As shown in Figs. 2(d) and 2(e), the largest eigenvalues of the RPA susceptibility tensor at different high-symmetry points (Γ, M, K, A) only show moderate enhancement with the increasing U, which are far from driving a CDW transition (marked by diverging susceptibility eigenvalue). We have further inspected the effects of inter-site Coulomb interactions (between Fe 3d and Ge 4p electrons), and still cannot find any instability mode that can lead to CDW state (see Fig. S3 in the SI). Therefore, we conclude that, in FeGe, e–e interactions alone cannot lead to a CDW-type Fermi surface instability; rather the CDW state results from a subtle interplay between on-site e–e interactions and electron–phonon couplings, which realizes an intriguing scenario of interaction-assisted phonon instability, giving rise to the CDW state.

As the phonon spectrum at $U = 4.1\,\text{eV}$ has a whole optical-phonon branch with imaginary frequencies within the $k_z = 0$ plane (Fig. 2), which implies that there could be various possible lattice distortions. Here we only consider the unstable phonon modes at the three M points in the pristine Brillouin zone, which are the modes that first become unstable as U increases. We first make a linear combination of the three unstable phonon modes at the three M points, which yield a 2×2 supercell structure. Then we take such a lattice distortion as an initial ansatz for the structural relaxation calculation. In Fig. 3(a) we present the fully relaxed lattice structure of a 2×2 supercell, which preserves all the symmetries of the pristine structure. This is a stable structure as no more imaginary frequency can be found in its phonon spectrum as shown in Fig. S8 in the SI. Such a 2×2 CDW phase involves two types of lattice distortions. The first one is a type of in-plane shortening or elongation of the nearest-neighbour Ge–Ge bond within the honeycomb Ge layer, which forms a Kekulé-type distortion pattern of the Ge honeycomb lattice as shown in the top panel of Fig. 3(a), where the two Ge atoms connected by a solid line denote the shortened Ge–Ge bond, consistent with the previous report.[38] The Kekulé distortions of the two Ge honeycomb layers within an antiferromagnetic primitive cell stacks along the z direction in an anti-phase way as illustrated by the opposite Kekulé distortions for the bottom and top Ge layers [top panel of Fig. 3(a)]. The second type of distortion is the out-of-plane buckling of the Ge atoms within the Fe kagome plane, as shown in the bottom panel of Fig. 3(a). Although the unstable phonon mode at M point may also lead to a 2×1 CDW state, it is inconsistent with the experimental observations.[34,35] Thus, the CDW phase observed in experiments may be the 2×2 supercell resulted from the spontaneous condensation of three unstable phonon modes at the three M points, which are characterized by in-plane Kekulé distortions and out-of-plane bucklings of the Ge atoms.

We then turn to the discussion of the electronic struc-

tures and orbital magnetic properties of antiferromagnetic FeGe within the CDW phase. In Fig. 3(b) we present the band structures of the antiferromagnetic FeGe in the 2×2 lattice structure, where every band is twofold degenerate due to the combined time-reversal ($\mathcal{T}$) and inversion symmetry of the antiferromagnetic phase. As mentioned above, a realistic Wannier tight-binding model including all the Fe $3d$ orbitals and Ge $4p$ orbitals has been constructed for the 2×2 antiferromagnetic CDW phase, based on which the inter-site currents have been calculated. As denoted by the arrows in Fig. 3(c), the current pattern of the Fe kagome layer with spin-up magnetization in the 2×2 CDW phase is qualitatively different from that of the pristine phase [Fig. 1(a)]. In the pristine phase of the antiferromagnetic state, the currents flow around a loop connecting the nearest neighboring Fe triangle within the kagome plane, with the current amplitude ~ 250 nA. In the 2×2 CDW phase, as a result of the lattice distortion, the current pattern within each Fe kagome layer consists of two types of current loops: the first one only flows between the nearest neighboring Fe sites, forming a star of David (SoD) current loop flowing in the clockwise direction [black arrows in Fig. 3(c)] with the current amplitude $\sim$360 nA; the second type only flows between the second nearest neighboring Fe sites, forming double triangular shaped (DT) current loops flowing in the counterclockwise direction [red arrows in Fig. 3(c)] with the current amplitude ~ 280 nA. These two types of current loops intersect with each other, forming an intriguing "current-loop density wave state" that is driven by the subtle interplay among magnetism, SOC, and the charge order. The current pattern in the Fe kagome layer with spin down magnetization is exactly opposite to that of the spin-up layer.

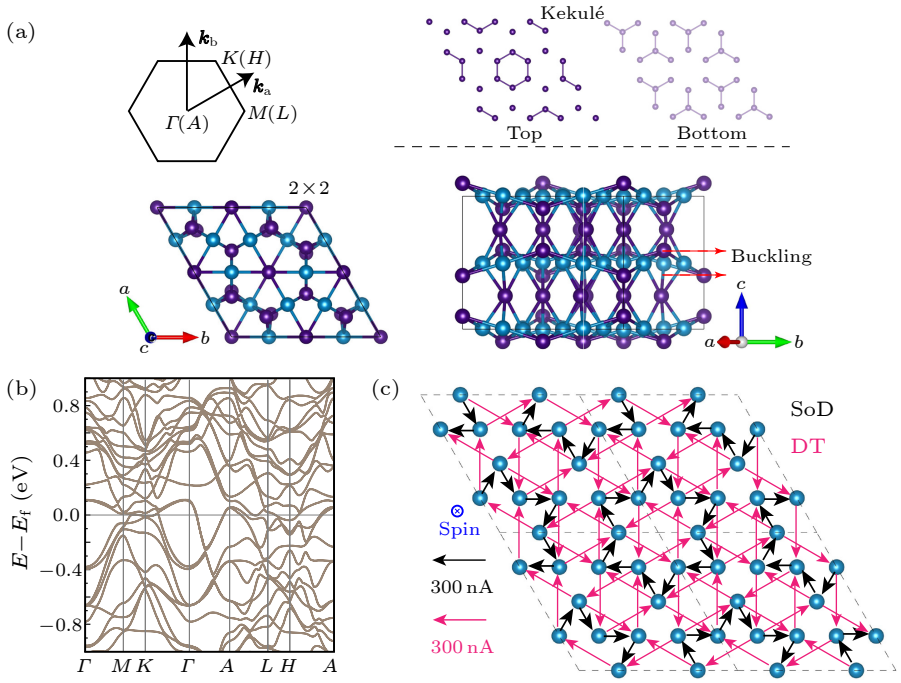

Fig. 3. Lattice structure, electronic structure, and current-loop states of the CDW phase of FeGe. (a) First Brillouin zone, relaxed lattice structure, illustration of the Kekulé structure, and buckling of the 2×2 CDW structure of FeGe. The Kekulé structure is formed by the distortion of the Ge atoms in the Ge planes. The lower-right panel is the side view to show the buckling of the Ge atoms in the kagome plane. (b) Band structures of the 2×2 supercell structure. (c) Current patterns of the 2×2 supercell structure, with only the spin-down layer shown here. SoD: star of David, DT: double triangular.

The current-loop state in FeGe can be captured by a simple tight-binding model. For a monolayer ferromagnetic kagome lattice, the tight-binding Hamiltonian can be written as

$$\hat{H}_{\text{mono}} = -t \sum_{\langle ij \rangle} \hat{c}_i^{\dagger} \hat{c}_j + i\lambda \sum_{\langle i\alpha, j\beta \rangle} (\boldsymbol{E}_{ij} \times \boldsymbol{r}_{ij})_z \cdot \boldsymbol{\sigma}_z^{\alpha\beta} \hat{c}_{i\alpha}^{\dagger} \hat{c}_{j\beta} + J \sum_{i\alpha\beta} \boldsymbol{S}_i \cdot \boldsymbol{\sigma}^{\alpha\beta} \hat{c}_{i\alpha}^{\dagger} \hat{c}_{i\beta}, \quad (1)$$

where $\langle\ \rangle$ refers to the nearest neighbor hopping, $\hat{c}_i^{\dagger}$ ($\hat{c}_j$) is the electron creation (annihilation) operator at site i (j), $\alpha\beta$ is the spin index. The first term is the usual first-neighbor hopping within the kagome triangles. The second term is the Kane–Mele-type SOC term [44] which is generated by the internal in-plane electric field $\boldsymbol{E}_{ij}$ normal to the bond vector $\boldsymbol{r}_{ij}$ connecting the two sites i and j (see the SI). The third term is the effective magnetic exchange interaction. If one periodically stacks the monolayer model along the z direction in an antiferromagnetic configuration with some proper interlayer coupling included, one would obtain a minimal model describing the electronic properties of antiferromagnetic FeGe in the pristine structure. Surprisingly, despite the complexity of the Fermi surface

topology in the pristine structure of FeGe [Figs. 1(b) and 2(b)], the current pattern from first principles calculations [Fig. 1(a)] is perfectly consistent with that obtained from the simple tight-binding theory described above. In general, more terms can be included into the model for a more realistic description of the system. For example, next-nearest-neighbor hoppings and SOC can be added, which can lead to the DT current pattern; and an effective charge order can also be added to the tight-binding model which give rises to the SoD current pattern. More details about the extensions of the tight-binding model can be found in the SI.

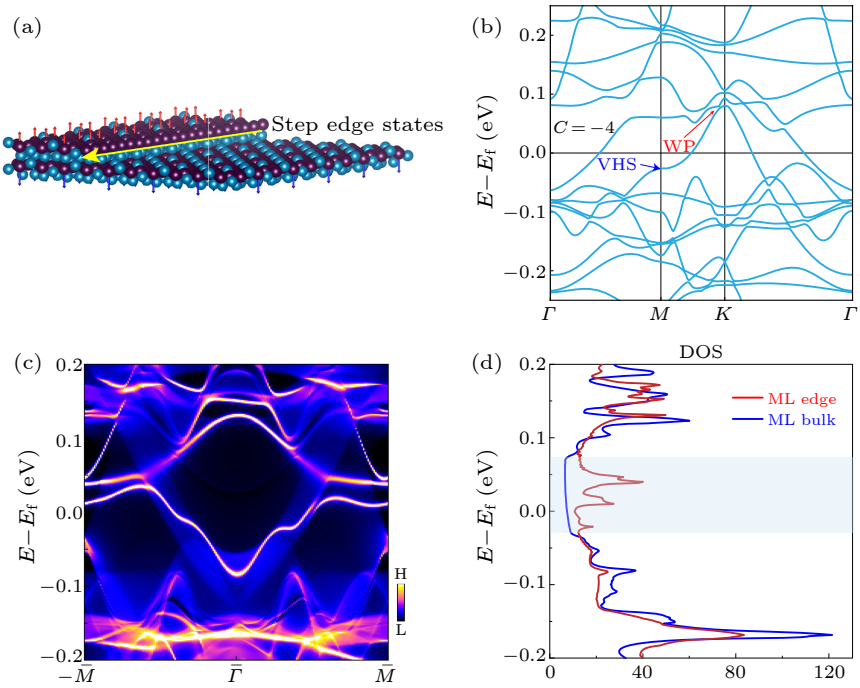

Fig. 4. Topological properties of the single kagome layer of the 2×2 supercell structure of FeGe. (a) Schematic of the step edge states of the 2×2 supercell structure of FeGe. (b) Band structures of monolayer FeGe. The Weyl point protected by $M_x\mathcal{T}$ symmetry is marked by WP along the K–M line. The van Hove singularity at the M point is marked by VHS. (c) Edge states. (d) DOS for the bulk and the edge of the single layer. ML bulk in (d) refer to the DOS of the bulk states of single kagome layer. ML edge refer to DOS of the edge states. The shading area in (d) refer to the gap region of the ML bulk DOS.

We note that in experiments, edge states [Fig. 4(a)] are observed when the bias voltage is within the gap range of the CDW structures,[34] indicating the topological nature of the antiferromagnetic CDW phase. To shed light on these observations, we calculate the band structures and edge states of the single kagome layer for the 2×2 structure. The band structures of the monolayer are shown in Fig. 4(b). We find that there exists both Weyl points (protected by $M_x\mathcal{T}$ symmetry) and topologically nontrivial Chern band near the Fermi level, which may lead to nontrivial edge states. As we can see from Fig. 4(c) that there exist prominent edge states for the single kagome layer. We further calculate both the edge and bulk DOS for the case of single kagome layer in Fig. 4(d). A gap feature can be clearly seen in the bulk DOS, while large edge states appear within the bulk (partial) gap, consistent with the experiments.[34]

To conclude, based on first principles calculations, we have systematically studied the electronic structures, Fermi-surface quantum fluctuations, as well as phonon properties of the antiferromagnetic kagome metal FeGe. We find that charge density wave emerges due to a subtle cooperation between e–e interactions and electron–phonon couplings, which leads to an unusual scenario of interaction-triggered phonon instabilities, and eventually yields a charge density wave state. We further show that, in the CDW phase of such an antiferromagnetic kagome metal, the ground-state current density distribution exhibits an intriguing star-of-David pattern, leading to flux density modulation, which can be potentially measured by neutron diffraction measurements. Such current loop pattern emerges as a result of the subtle interplay between magnetism, lattice geometry, charge order, and SOC, which can be described by a simple, yet universal, tight-binding theory including a Kane–Mele-type SOC term and a magnetic exchange interaction. We further study the origin of the peculiar step-edge states in FeGe, which sheds light on the topological properties in this new type of kagome antiferromagnetic material.

Acknowledgments. We thank Quansheng Wu and Xiangang Wan for valuable discussions. This work was supported by the National Natural Science Foundation of China (Grant No. 12174257), the National Key R & D program of China (Grant No. 2020YFA0309601), the Science and Technology Commission of the Shanghai Municipality (Grant No. 21JC1405100), and the Start-Up Grant of

ShanghaiTech University.

References

[1] Bergman D L, Wu C, and Balents L 2008 *Phys. Rev. B* **78** 125104
[2] Zhou Y, Kanoda K, and Ng T K 2017 *Rev. Mod. Phys.* **89** 025003
[3] Neupert T, Denner M M, Yin J X, Thomale R, and Hasan M Z 2022 *Nat. Phys.* **18** 137
[4] Yin J X, Lian B, and Hasan M Z 2022 *Nature* **612** 647
[5] Kiesel M L, Platt C, and Thomale R 2013 *Phys. Rev. Lett.* **110** 126405
[6] Wang W S, Li Z Z, Xiang Y Y, and Wang Q H 2013 *Phys. Rev. B* **87** 115135
[7] Yu S L and Li J X 2012 *Phys. Rev. B* **85** 144402
[8] Yin J X, Zhang S S, Li H *et al.* 2018 *Nature* **562** 91
[9] Ye L D, Kang M G, Liu J W *et al.* 2018 *Nature* **555** 638
[10] Liu E, Sun Y, Kumar N *et al.* 2018 *Nat. Phys.* **14** 1125
[11] Yin J X, Ma W, Cochran T A *et al.* 2020 *Nature* **583** 533
[12] Ko W H, Lee P A, and Wen X G 2009 *Phys. Rev. B* **79** 214502
[13] Xu G, Lian B, and Zhang S C 2015 *Phys. Rev. Lett.* **115** 186802
[14] Wu X, Schwemmer T, Müller T *et al.* 2021 *Phys. Rev. Lett.* **127** 177001
[15] Feng X L, Jiang K, Wang Z Q, and Hu J P 2021 *Sci. Bull.* **66** 1384
[16] Park T, Ye M, and Balents L 2021 *Phys. Rev. B* **104** 035142
[17] Ortiz B R, Teicher S M, Hu Y *et al.* 2020 *Phys. Rev. Lett.* **125** 247002
[18] Jiang Y X, Yin J X, Denner M M *et al.* 2021 *Nat. Mater.* **20** 1353
[19] Zhao H, Li H, Ortiz B R, Teicher S M L, Park T, Ye M, Wang Z, Balents L, Wilson S D, and Zeljkovic I 2021 *Nature* **599** 216
[20] Chen H, Yang H, Hu B *et al.* 2021 *Nature* **599** 222
[21] Kang M G, Fang S, Kim J K *et al.* 2022 *Nat. Phys.* **18** 301
[22] Yu L, Wang C, Zhang Y *et al.* 2021 arXiv:2107.10714 [cond-mat.supr-con]
[23] Liu Z H, Zhao N N, Yin Q W *et al.* 2021 *Phys. Rev. X* **11** 041010
[24] Cho S, Ma H, Xia W *et al.* 2021 *Phys. Rev. Lett.* **127** 236401
[25] Nie L P, Sun K L, Ma W R *et al.* 2022 *Nature* **604** 59
[26] Mielke C, Das D, Yin J X *et al.* 2022 *Nature* **602** 245
[27] Li H, Zhao H, Ortiz B R, Park T, Ye M, Balents L, Wang Z, Wilson S D, and Zeljkovic I 2022 *Nat. Phys.* **18** 265
[28] Shan Z Y, Biswas P K, Ghosh S K *et al.* 2022 *Phys. Rev. Res.* **4** 033145
[29] Liu J P, Park S Y, Garrity K F, and Vanderbilt D 2016 *Phys. Rev. Lett.* **117** 257201
[30] Liu J P and Dai X 2021 *Nat. Rev. Phys.* **3** 367
[31] Bourges P, Bounoua D, and Sidis Y 2021 *C. R. Phys.* **22** 7
[32] Denner M M, Thomale R, and Neupert T 2021 *Phys. Rev. Lett.* **127** 217601
[33] Ma H Y, Yin J X, Hasan M Z, and Liu J 2022 *Phys. Rev. B* **106** 155125
[34] Yin J X, Jiang Y X, Teng X *et al.* 2022 *Phys. Rev. Lett.* **129** 166401
[35] Teng X K, Chen L, Ye F *et al.* 2022 *Nature* **609** 490
[36] Teng X, Oh J S, Tan H X *et al.* 2023 *Nat. Phys.* **19** 814
[37] Miao H, Zhang T T, Li H X *et al.* 2023 *Nat. Commun.* **14** 6183
[38] Shao S, Yin J X, Belopolski I *et al.* 2023 *ACS Nano* **17** 10164
[39] Zhou H, Yan S, Fan D, Wang D, and Wan X 2023 *Phys. Rev. B* **108** 035138
[40] Wu L, Hu Y, Fan D, Wang D, and Wan X 2023 *Chin. Phys. Lett.* **40** 117103
[41] Bernhardt J, Lebech S B, and Beckman O 1984 *J. Phys. F* **14** 2379
[42] Cococcioni M and de Gironcoli S 2005 *Phys. Rev. B* **71** 035105
[43] Giustino F 2017 *Rev. Mod. Phys.* **89** 015003
[44] Kane C L and Mele E J 2005 *Phys. Rev. Lett.* **95** 146802